U.S. DEPARTMENT OF THE INTERIOR
U.S. GEOLOGICAL SURVEY

GEOLOGIC INVESTIGATIONS
MAP I–2591
Pamphlet accompanies map

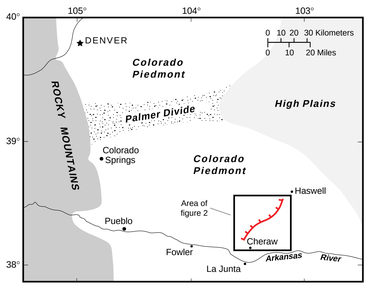

Figure 1. Index map showing location of Cheraw fault (hachured red line) on the Colorado Piedmont about 100 km east of the Rocky Mountains.

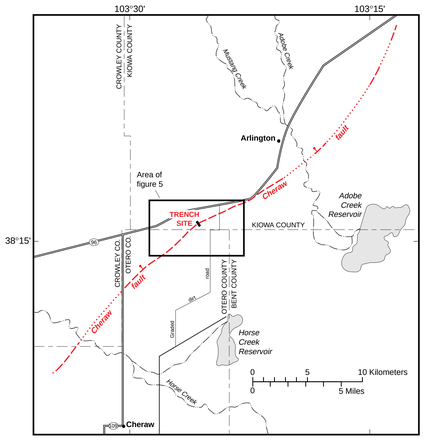

Figure 2. Aerial map of the Cheraw fault (heavy red line) showing selected geographic and cultural features. Bar and ball on downthrown side of fault. Fault is dashed where approximately located and dotted where concealed.

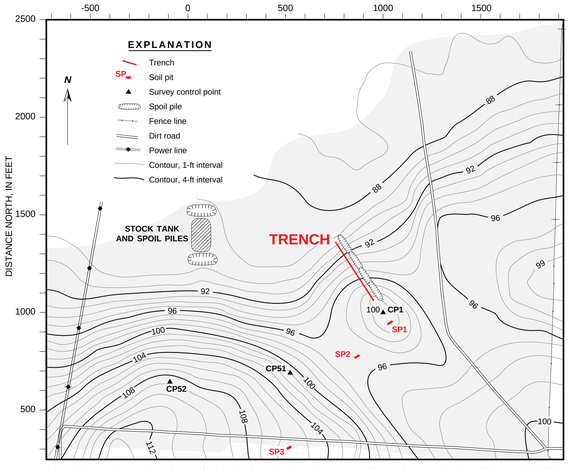

Figure 3. Topographic map showing location of trench and soil pits. Shaded area shows coverage of topographic survey. Trench is in SE 1/4 sec. 34, T. 20 S., R. 54 W., USGS Houston Lakes 7.5-minute quadrangle, Colorado. Control point CP1 is assigned an arbitrary elevation of 100 feet, at an arbitrary position of 1000 feet north and 1000 feet east.

MAPPED PART OF SOUTHWEST WALL OF TRENCH ACROSS CHERAW FAULT

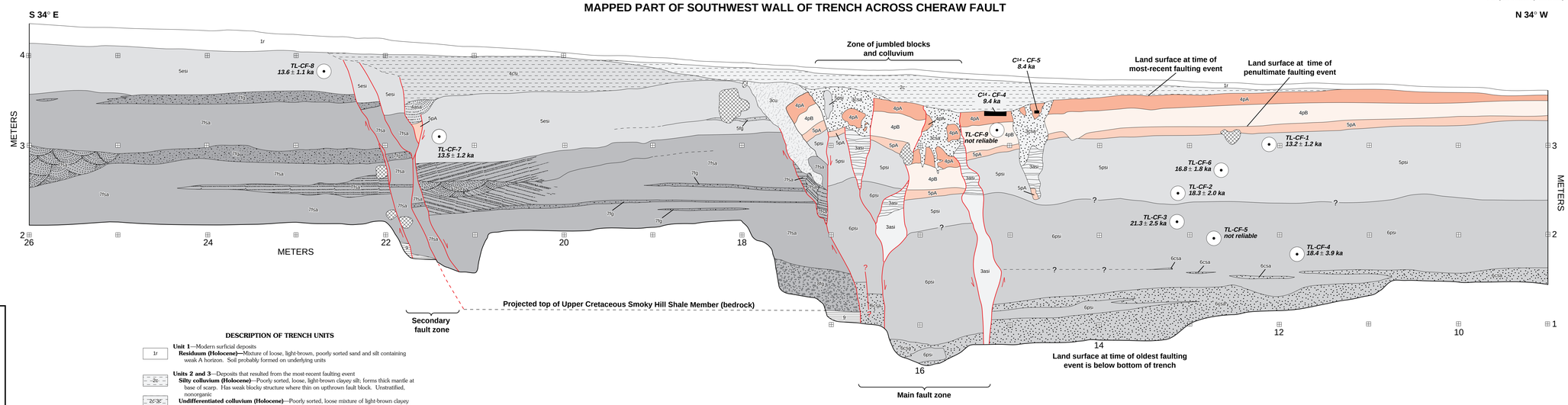

DESCRIPTION OF TRENCH UNITS

Unit 1—Modern surficial deposits

1r — **Residuum (Holocene)—**Mixture of loose, light-brown, poorly sorted sand and silt containing weak A horizon. Soil probably formed on underlying units

Units 2 and 3—Deposits that resulted from the most-recent faulting event

2c — **Silty colluvium (Holocene)**—Poorly sorted, loose, light-brown clayey silt; forms thick mantle at base of scarp. Has weak blocky structure where thin on upthrown fault block. Unstratified, noncarganic

2c-3c — **Undifferentiated colluvium (Holocene)**—Poorly sorted, loose mixture of light-brown clayey silt and intact blocks of sediment derived from upthrown fault block. Unit 2 and all subunits of unit 3 mapped on southwest trench wall. Combination of units 2 and 3 mapped on northeast wall of trench

3sa-a — **Sandy colluvium (Holocene)**—Moderately well sorted, loose, very light brown silty sand; probably reworked eolian material. Fills fissures and irregular topography formed by ground rupturing during most-recent faulting event

3cu — **Undifferentiated colluvium (Holocene)**—Heterogeneous mixture of poorly sorted clayey silt (reworked units 5 and 6) and colluvial collapse blocks too small to map separately. Only mapped along main fault on southwest wall of trench

3asi — **Silty alluvium (Holocene)**—Poorly sorted, loose, brown sandy silt that fills elongate fissures. Upper part of unit typically has thin layers of light-brown sand that give the unit a bedded appearance (see symbols)

3asa — **Sandy alluvium (Holocene)**—Poorly sorted, loose, very light brown sandy alluvium that fills openings between disturbed blocks of silt (units 5 and 6). Typically unbedded, but one area on the northeast trench wall has crossbedding that is characteristic of deposition by flowing water (see symbols)

Unit 4—Deposits that resulted from the penultimate faulting event

4pA — **Soil A horizon (Holocene and upper Pleistocene)**—Organic-rich A horizon developed on paludal silts deposited at base of fault scarp. Bulk organic carbon and charcoal extracted from this horizon yielded radiocarbon dates as reported in table 1

4pB — **Soil B horizon (upper Pleistocene)**—Slightly oxidized layer (cambic B horizon) developed in paludal silts deposited at base of fault scarp

4csi — **Silty colluvium (upper Pleistocene)**—Homogeneous light- to medium-brown clayey silt; unbedded, friable to hard (where dry). Interpreted as colluvium reworked from unit 5 on upthrown fault block. As such, it is related to the most-recent faulting event on the southern (secondary) fault zone

4sa — **Sandy alluvium (upper Pleistocene)**—Poorly sorted, loose, very light brown sandy alluvium that fills a small graben at the southern (secondary) fault zone. Has crossbedding that is characteristic of deposition by flowing water (see symbols)

Unit 5—Deposits that resulted from the oldest faulting event in trench

5pA — **Soil A horizon (upper Pleistocene)**—Organic-rich, brown A horizon developed on paludal silts deposited at base of fault scarp. Bulk organic carbon extracted from this horizon yielded a radiocarbon date as reported in table 1. Locally, weak cambic B horizon is present below this unit but it was not mapped because of its subtle character

5esi — **Eolian silt (upper Pleistocene)**—Brown sandy silt (loess) and fine- to medium-grained sand; massive. Mainly eolian deposit but may contain some colluvium; transitional and probably coeval with unit 5psi

5psi — **Paludal silt (upper Pleistocene)**—Brown silt; massive when moist, blocky when dry. Upper of two thick (0.4–1.1 m) silt layers (eolian?) deposited in marshes or ephemeral lakes that formed at the base of the fault scarp, probably as a result of backtilting. Later sedimentation overlapped the fault zone. Basal contact of unit was defined on the basis of blocky structure and may not be stratigraphically significant

5fg — **Fluvial gravel (upper Pleistocene)**—Thin lens of sandy pebble gravel that is interbedded with paludal silt (unit 5psi). Unit represents occasional fluvial deposition at base of scarp

Unit 6—Deposits that resulted from the oldest faulting event in trench

6psi — **Paludal silt (upper Pleistocene)**—Brown to dark-brown, massive silt. Lower of two thick (0.6–1.3 m) silt layers (eolian?) deposited in marshes or ephemeral lakes that formed at the base of the fault scarp, probably as a result of backtilting. Unit is restricted to downthrown fault block. Base is interbedded with fault-scarp colluvium (unit 6csa)

6csa — **Sandy colluvium (upper Pleistocene)**—Unbedded to poorly bedded, light-brown, fine- to medium-grained sand interbedded with the basal part of unit 6psi. Lack of bedding and presence of gravel clasts suggest that the unit is derived from the erosion of unit 7 on the upthrown fault block. Grades downward into unit 7 in auger holes and where exposed in trench during excavation

Units 7 and 8—Deposits that predate the oldest faulting event in trench

7?sa — **Fluvial sand (upper Pleistocene)**—Interbedded light-brown, fine- to medium-grained sand and minor beds of sandy pebble gravel. Sandy gravels are moderately to well sorted and indicate stream deposition. Bedding forms in fluvial sand are stratified, planar, and crossbedded (see symbols) although some thick sandy parts of unit are massive

7fg — **Fluvial gravel (upper Pleistocene)**—Light-brown, fine- to medium-grained sandy gravel. Moderately well sorted. Contains 5- to 10-cm-diameter clasts reworked from older Quaternary and Pliocene alluvium (Rocky Flats and Nussbaum Alluviums; Sharps, 1976) in upper part of drainage area. Pebble imbrication and bedforms indicate a southerly transport direction

7cfg — **Fluvial gravel (upper Pleistocene)**—Poorly sorted sandy alluvium containing angular to subrounded, pebble- to cobble-size clasts of shale (bedrock). Clast shape and monolithologic composition indicate short transport distances by a stream. Unit predates the three events recorded in trench

Unit 9—Bedrock

9 — **Smoky Hill Shale Member of the Niobrara Formation (Upper Cretaceous)**—Orangish-brown to olive-green shale; gypsiferous, thinly bedded. Exposed in lower 0.5 m of uplifted (southern) block, adjacent to main and secondary fault zones in trench

EXPLANATION OF TRENCH SYMBOLS

Faults—Arrows indicate relative sense of motion. Dashed where inferred, queried where uncertain

Stratigraphic contacts—Dashed where subtle or gradational. Queried where inferred. Note: contacts between units 2 and 3 and older units result from deposition of younger colluvium and alluvium against exposed fault planes

Area sampled for radiocarbon (C¹⁴) analysis and estimated age of faulting event—See table 1

Thermoluminescence sample and estimated age—See table 2

Crudely bedded

Crossbedded

Planar bedded

Krotovina (fossil animal burrow)

Location of horizontal and vertical control points (1 meter grid)

CORRELATION OF TRENCH UNITS

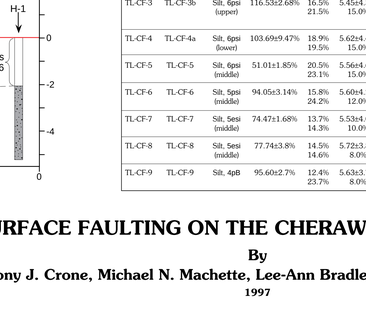

MAPPED PART OF NORTHEAST WALL OF TRENCH ACROSS CHERAW FAULT (mirror image)

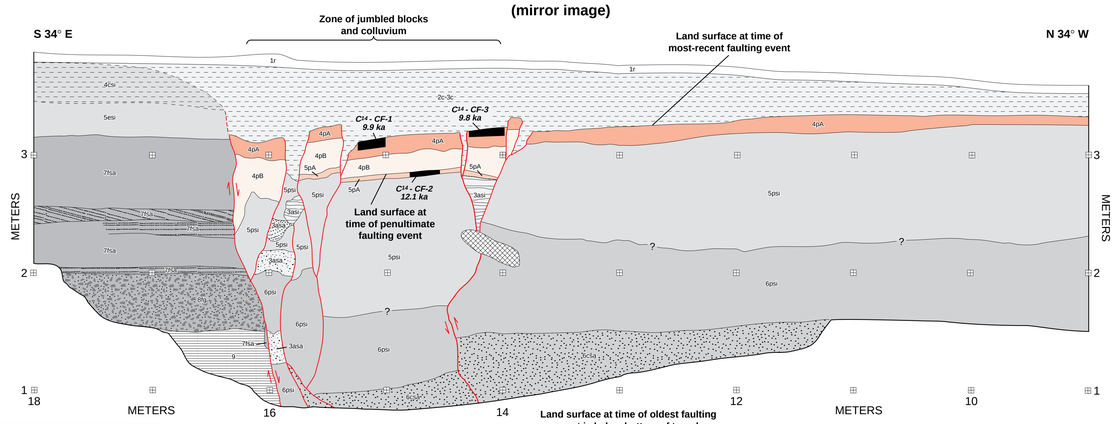

Table 1. *Data for radiocarbon dating of samples from trench across the Cheraw fault*

[Measured, conventional, and calibrated ages are reported as yr B.P., with reference to 1950. The estimated time of faulting events is calculated by subtracting the apparent mean residence time of sampled material from dendrochronologically calibrated age, and reported as yr B.P. Estimated times shown in bold are those used in discussion and mapped parts of trench. See text for discussion of apparent mean residence time. Dendrochronological calibration is not available for samples that have conventional radiocarbon ages greater than about 10,000 years, but radiocarbon ages in the range of 10,700 yr (C^{14}-CF-2) typically have a calendric age of about 12,600 yr B.P. (Stuiver and Reimer, 1993; Lowell and Teller, 1994). NA, not applicable]

Field sample No.	Laboratory sample No.	Sampled material, unit	Measured age, yr B.P. ±1σ	C^{13}/C^{12} ratio ‰	Conventional age, C^{14} yr B.P. ±1σ	Calibrated age and ±2σ range, yr B.P.	Apparent mean residence time, in yr	Estimated time of faulting event and ±2σ range (yr B.P.)
C^{14}-CF-1	Beta-93290	Soil organics, 4pA	9,260±90	-15.4	9,420±90	10,390 10,180-10,635 10,730-10,865	500	Event 1: <9,890 (<**9.9 ka**) 9,680-10,135 10,230-10,365
C^{14}-CF-2	Beta-93291	Soil organics, 5pA	10,550±100	-15.7	10,700±100	ca. 12,600	500	Event 2: ca. <12,100 (<**12.1 ka**)
C^{14}-CF-3	Beta-93552	Soil organics, 4pA	9,160±90	-15.4	9,320±90	10,320 10,165-10,330	500	Event 1: <9,820 (<**9.8 ka**) 9,665-9,830
C^{14}-CF-4	Beta-93553	Soil organics, 4pA	8,650±90	-15.7	8,880±90	9,865 9,525-9,970	500	Event 1: <9,365 (<**9.4 ka**) 9,025-9,470
C^{14}-CF-5	Beta-83716	Charcoal, 4pA	7,730±50	-27.1	7,690±50	8,415 8,390-8,445	NA	Event 1: <8,415 (<**8.4 ka**) 8,390-8,445

Table 2. *Data for thermoluminescence age estimates of samples from trench across the Cheraw fault*

Field sample No.	Laboratory sample No.	Sampled material, unit	Environmental dose, Greys	Moisture content: field, saturation	Dose rate: Greys ± 1σ at moisture content	Total bleach TL age, ka ±2σ (A)	Partial bleach TL age, ka ±2σ (B)	Favored TL age, ka ±2σ (A)
TL-CF-1	TL-CF-1	Silt, 5psi (upper)	74.93±1.74%	15.5% 24.3%	5.66±4.1% 12.0%	13.2±1.2	12.0±3.6	13.2±1.2 (A)
TL-CF-2	TL-CF-2	Silt, 5psi (lower)	104.56±3.31%	14.5% 17.4%	5.72±4.2% 12.0%	18.3±2.0	18.0±3.1	18.3±2.0 (A)
TL-CF-3	TL-CF-3a	Silt, 6psi (upper)	115.36±5.18%	16.5% 21.5%	5.45±4.3% 15.0%	21.2±2.9	15.5±13.4	21.3±2.5 (A, average of -3a,- 3b)
TL-CF-3	TL-CF-3b	Silt, 6psi (upper)	116.53±2.68%	16.5% 21.5%	5.45±4.3% 15.0%	21.4±2.2	21.3±16.7	21.3 ±2.5 (A, average of -3a,- 3b)
TL-CF-4	TL-CF-4a	Silt, 6psi (lower)	103.69±9.47%	18.9% 19.5%	5.62±4.4% 15.0%	18.4±3.9	16.2±10.5	18.4±3.9 (A)
TL-CF-5	TL-CF-5	Silt, 6psi (middle)	51.01±1.85%	20.5% 23.1%	5.56±4.6% 15.0%	9.2±0.9	5.1±1.5	Not reliable (A)
TL-CF-6	TL-CF-6	Silt, 5psi (middle)	94.05±3.14%	15.8% 24.2%	5.60±4.2% 12.0%	16.8±1.8	20.4±3.1	16.8±1.8 (A)
TL-CF-7	TL-CF-7	Silt, 5esi (middle)	74.47±1.68%	13.7% 14.3%	5.53±4.0% 10.0%	13.5±1.2	12.8±1.3	13.5±1.2 (A)
TL-CF-8	TL-CF-8	Silt, 5esi (middle)	77.74±3.8%	14.5% 14.6%	5.72±3.8% 8.0%	13.6±1.1	11.5±1.1	13.6±1.1 (A)
TL-CF-9	TL-CF-9	Silt, 4pB	95.60±2.7%	12.4% 23.7%	5.63±3.7% 8.0%	17.0±1.6	16.4±1.5	Not reliable (A)

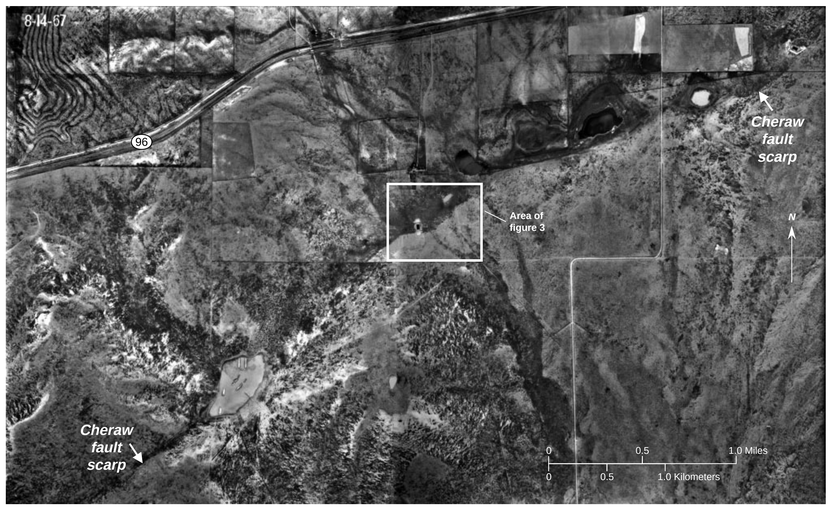

Figure 5. Computer-scanned composite of two aerial photographs showing the Cheraw fault scarp near the trench site. Photographs are CNW-SHH-118 (left) and CNW-SHH-112 (right) taken on August 14, 1967 (U.S. Department of Agriculture. Agricultural Stabilization and Conservation Service). Colorado State Highway 96 is present in the northwest corner of the image.

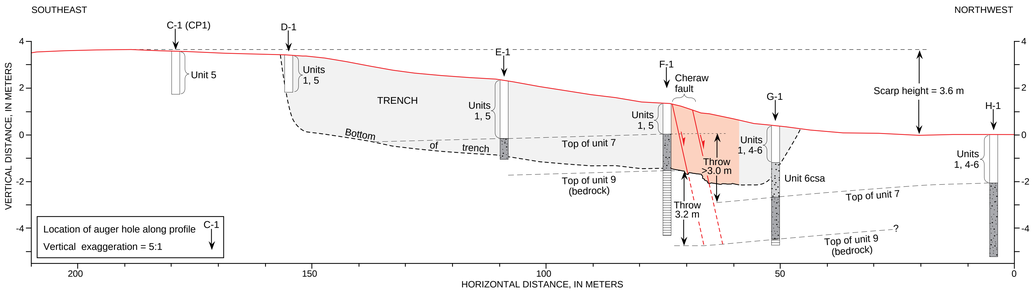

Figure 4. Profile of fault scarp at the trench site (heavy solid red line); line of profile coincides with center of trench. Red shaded area shows mapped portion of trench. See description and explanation of trench units for patterns in auger holes.

LATE QUATERNARY SURFACE FAULTING ON THE CHERAW FAULT, SOUTHEASTERN COLORADO

By

Anthony J. Crone, Michael N. Machette, Lee-Ann Bradley, and Shannon A. Mahan

1997

Manuscript approved for publication October 8, 1996

Any use of trade names in this publication is for descriptive purposes only and does not imply endorsement by the U.S. Geological Survey

For sale by U.S. Geological Survey Information Services, Box 25286, Federal Center, Denver, CO 80225

U.S. DEPARTMENT OF THE INTERIOR
U.S. GEOLOGICAL SURVEY

LATE QUATERNARY SURFACE FAULTING ON THE CHERAW FAULT, SOUTHEASTERN COLORADO

By

Anthony J. Crone, Michael N. Machette, Lee-Ann Bradley,
and Shannon A. Mahan

Pamphlet to accompany
GEOLOGIC INVESTIGATIONS
MAP I–2591

CONTENTS

INTRODUCTION

Although relatively infrequent, earthquakes can unexpectedly occur in the stable interior of continents such as the midwestern part of the United States and can cause damage, injuries, and fatalities in populated regions (Johnston and Kanter, 1990). This study of the Cheraw fault in southeastern Colorado is part of an ongoing effort to better understand the long-term behavior of potentially seismogenic faults in the interior of continental plates where the historical rates of seismicity are low compared to plate-margin settings (Johnston, 1994).

For decades, earthquake-hazard assessments in stable continental regions such as the central and eastern United States have been based largely on the assumption that the spatial distribution of historical seismicity is an accurate guide to the location of future large, potentially devastating earthquakes. However, data from recent historical earthquakes coupled with paleoseismologic studies of faults in the stable interior of North America (Crone and Luza, 1990) and Australia (Crone and others, 1992; Machette and others, 1993) indicate that modern seismicity is *not* a reliable indicator of all potentially hazardous faults that might rupture in the future. These studies show that some potentially active faults are currently aseismic and may have remained so for many tens of thousands of years. After a lengthy period of quiescence and with little or no precursory activity, these faults may generate moderate- to large-magnitude earthquakes that are associated with as much as 35 km of surface rupture. Thus, studies that document the history of movement on Quaternary faults in stable continental regions are needed to characterize both their short-term and long-term behavior and to improve hazard assessments in these largely aseismic areas.

Earthquake-hazard assessments in stable continental regions are hindered by an incomplete inventory of prehistoric surface ruptures. For many years, little consideration was given to the possibility that prehistoric Quaternary surface-rupturing earthquakes had occurred in the stable interior of the United States. However, in the early 1980's, a Quaternary scarp was recognized on the Meers fault in southwestern Oklahoma, and subsequent studies documented evidence of two Holocene surface-faulting events (Crone and Luza, 1990; Kelson and Swan, 1990). The study described herein establishes the Cheraw fault as the second aseismic fault in the stable interior of the west-central United States to have demonstrable late Quaternary offset. We suspect that additional studies in the continental interior will identify other faults that have moved in the recent geologic past and that could generate damaging earthquakes in the future.

The main purpose of this report is to present the basic stratigraphic evidence and numerical ages that document Holocene and latest Pleistocene surface-faulting events on the Cheraw fault. The results reported here expand upon and supersede the findings reported by Crone and Machette (1995). The evidence for the number and timing of faulting events is derived from several sources of information including detailed topographic mapping of our study site, subsurface stratigraphy determined from a series of 1.5- to 7.6-m-deep auger holes, a 110-m-long exploratory trench, and analysis of samples for radiocarbon and thermoluminescence dating.

GEOLOGIC AND SEISMOLOGIC FRAMEWORK

The Cheraw fault was recognized during regional geologic mapping by the U.S. Geological Survey more than 25 years ago (Scott, 1970; Sharps, 1976; Kirkham and Rogers, 1981), but no detailed paleoseismological studies were conducted perhaps because of the fault's relatively remote location. The fault is about 100 km east of Pueblo, Colo. (the closest major urban area), and about 140 km east of the range front of the Rocky Mountains. The fault is within a sparsely populated portion of the Colorado Piedmont (fig. 1). It trends N. 45° E., has a down-to-the-northwest sense of throw, and has a mapped length of about 44 km. In many places, the fault's trace is mapped as approximately located, inferred, or concealed (Sharps, 1976). Along its central part, the fault displaces early Quaternary piedmont surfaces (mainly formed by early Pleistocene Rocky Flats Alluvium; Scott, 1982) that are widespread in southeastern Colorado, and in a few locations including where we excavated our exploratory trench, movement of the fault formed a scarp on late Pleistocene deposits.

Historical seismicity of southeastern Colorado is sparse, and no historical events can be directly associated with the Cheraw fault. The most notable earthquake in the region was an intensity IV event in November 1955, located 25–30 km northwest of La Junta, Colo., and about 25 km west-southwest of the trench site (Kirkham and Rogers, 1981). Thus, the record of historical seismicity offers no insight into the seismogenic potential of the fault, as is the case with many intraplate Quaternary faults.

BEDROCK GEOLOGY

Sharps (1976) mapped the Cheraw fault as primarily exposed in the Upper Cretaceous Smoky Hill Shale Member of the Niobrara Formation and showed it as inferred beneath Quaternary alluvium in several localities. However, Scott (1970) and Kirkham and Rogers (1981) interpreted discordant elevations of the Rocky Flats Alluvium across the fault as evidence of Quaternary movement. There is little evidence that throw on the fault has substantially offset the bedrock (tens of meters), thus the fault does not appear to have a long history of recurrent movement. For example, the cumulative throw on the fault is probably less than the thickness of the Smoky Hill Shale Member (150–215 m thick in the area) because neither the Fort Hays Limestone Member nor the Pierre Shale (all Upper Cretaceous), which are strati-

graphically below and above the Smoky Hill Shale Member, respectively, are exposed along the fault. Similarly, Sharps' (1976) structure-contour map shows only about 20–25 ft (6–8 m) of normal, down-to-the-northwest displacement on the fault, even though drill-hole control for the structure-contour map is relatively sparse in this area. Therefore, stratigraphic relations of bedrock units suggest that the Cheraw fault does not have a long (that is, Neogene) history of movement. Furthermore, stratigraphic data from shallow auger holes indicate that only about 7–8 m of cumulative Quaternary offset has occurred since deposition of the early Pleistocene Rocky Flats Alluvium (Crone and Machette, 1995).

SURFACE EXPRESSION OF THE FAULT

Where expressed in the field, the Cheraw fault typically forms a subtle, northwest-facing escarpment that is most recognizable where it opposes the regional topographic gradient (fig. 2), which slopes to the southeast toward the Arkansas River, some 30 km to the south (fig. 1). Aerial photographs clearly show areas where alluvium is ponded against the scarp because the scarp has dammed local drainages. Eolian processes were active in eastern Colorado, particularly during the Holocene (Madole, 1994) and latest Pleistocene, and in many places the scarp has been mantled by windblown sand and loess. Thus, in some low-lying areas along the fault's trace, material has preferentially accumulated on the downthrown (northwest) side of the scarp, so the scarp height is only a fraction of the actual throw due to a combination of erosion and deposition. The highest and oldest scarps, which record the longest history of faulting, are about 7–8 m high and are formed on the Rocky Flats Alluvium (mapped by Sharps, 1976).

The trenching study results indicate that eolian deposition has subdued the scarp's morphology. At the trench site where we document Holocene surface rupture, the scarp has a maximum slope angle of about 11° and a height of about 3.6 m. Based on fault-scarp morphology studies (Bucknam and Anderson, 1979), this scarp's morphology is much more subdued than comparable Holocene fault scarps in climatically similar parts of the Basin and Range Province in Utah. However, this comparison is complicated by the fact that the Cheraw scarp is the product of multiple surface-faulting events, whereas the Utah scarps result from single events. Nevertheless, partial burial of the Cheraw scarp by eolian deposits and by alluvium ponded on the downthrown side has resulted in a subdued morphology that makes it appear to be an older feature than was documented by the trenching study.

DESCRIPTION OF THE TRENCH SITE

In order to assess the location of the fault relative to the local topography, we made a detailed topographic map of the Cheraw trench site (fig. 3) by measuring 915 topographic data points in an area of approximately 0.4 km^2 using a Sokkia Set 5A Total Station. We contoured these data using commercial software (MacGridzo) to generate a detailed topographic map (fig. 3) with 1-foot (30-cm) contours; this map documents the location of the trench, scarp, and soil pits relative to cultural features (mainly roads and fences), which are the only notable landmarks in the area.

The scarp at the trench site is 3.6 m high and about 120 m wide (figs. 3 and 4). In late 1994, we excavated a 110-m-long, northwest-southeast-oriented trench across the scarp, and in 1995, we completed mapping of critical portions of the trench (fig. 4). The trench is located in the $SE^1/_4$ sec. 34, T. 20 S., R. 54 W. (USGS Houston Lakes 7.5-minute quadrangle), Kiowa County, Colo., on the property of the Timberlake Grazing Association. We selected this trench site because it is along part of the fault where a prominent scarp is present on Quaternary deposits that are inset into, and therefore substantially younger than, the Rocky Flats Alluvium. Aerial photographs (fig. 5) of the trench site show the presence of distinct fluvial channels (relatively dark areas) on the upthrown side of the scarp that define a through-flowing drainage system, which was disrupted by movement on the fault. The sharpness of these abandoned channels in the photographs suggest that they are likely late Pleistocene in age rather than middle Pleistocene or older. Thus, on the basis of our aerial photographic interpretations, we suspected that a detailed trenching study at this site would provide evidence for late Pleistocene or younger movement on the fault.

We started to excavate the trench near the crest of the broad scarp and anticipated intercepting one or more faults near the mid-portion of the scarp (fig. 4). However, the first fault (most headward in the trench) was not encountered until about 85 m from the beginning of the excavation (secondary fault zone at 22-m mark on mapped part of southwest wall of trench), and the main fault zone was intercepted 5–6 m farther downslope. The location of the faults relatively close to the base of the scarp is unusual, although in retrospect their location might have been expected owing to pervasive burial of the downthrown fault block (northwest side of fault). Nevertheless, all of the pertinent stratigraphic and structural details of the faulting were exposed in the northwesternmost 25 m of the trench, which is the portion that we mapped in detail and most of which is illustrated on the accompanying plate.

We systematically examined the entire trench several times for evidence of deformation, and ultimately confirmed that faulting was present only in the northwestern part shown on the plate. We carefully cleaned both walls of this part of the trench with mason's trowels to clarify and highlight the stratigraphic relations. Next we established a grid of string lines on both walls to use as a frame of reference for mapping. We identified key stratigraphic units and structural features on the walls and marked those features using multicolored tape. We then

mapped the features at a scale of 2 inches to 1 meter (approximate scale of 1:19.7). Finally, we described and sampled the stratigraphic units and collected samples for radiocarbon and thermoluminescence analyses.

TRENCH STRATIGRAPHY

The trench exposed distinctly different stratigraphy on the southeastern (upthrown) and the northwestern (downthrown) sides of the fault zones. Southeast of the main fault zone, the trench exposed a sequence comprised of bedrock (unit 9), overlain by fluvial sand and gravel (units 7 and 8), and capped by massive, sandy silt and fine- to medium-grained sand (units 5esi and 4csi). The bedrock is gypsiferous shale of the Smoky Hill Shale Member of the Niobrara Formation, which was exposed at the bottom of the trench on the southeastern side of the two fault zones. A poorly sorted fluvial gravel (unit 8fg) that contains abundant rip-up clasts of the shale is directly above the bedrock at the main fault zone. Upward, medium- to coarse-grained fluvial sand (unit 7sa) and gravel (unit 7fg) dominate; stratification in these units varies locally from well stratified to crossbedded to cut-and-fill structures. This entire sequence is capped by eolian silt (loess; unit 5esi) and, between the main and secondary fault zones, a wedge of colluvial silt (unit 4csi).

On the northwestern (downthrown) side of the main fault zone, the trench exposed a sequence of deposits that we interpret as a mixture of scarp-derived colluvium and fine-grained alluvium that accumulated in relatively moist, occasionally marshy (paludal) conditions at the base of the scarp. The oldest deposit exposed on the downthrown side was a massive, fine- to medium-grained sand (unit 6csa) that we interpret as scarp colluvium. This colluvium is overlain by and interfingers with massive silt (unit 6psi) and massive to blocky silt (unit 5psi) that we interpret as paludal deposits, which were ponded against the scarp. Much of the silt in these paludal deposits is probably reworked loess that originally mantled the landscape during the late Pleistocene. Unit 5psi is capped by a moderate to weakly developed A horizon (unit 5pA), which formed during a time when the sedimentation rate at the base of the scarp was relatively low and the surrounding landscape was relatively stable. On the northwestern side of the main fault zone, the A horizon on unit 5 is buried by paludal silt that contains a lower B horizon (unit 4pB) and an upper A horizon (unit 4pA). Between the main fault zone and the secondary fault zone, unit 5 is buried by sandy alluvium (unit 4asa) and silty colluvium (unit 4csi) that we interpret as debris, which accumulated along the scarp at the same time as the paludal silt was collecting in the adjacent marsh lower on the slope. Units 3 and 2 are sandy alluvium and silty colluvium that locally fill fissures and form wedge-shaped deposits of scarp colluvium derived from erosion of the fault scarp and adjacent scarp slope. In places within the main fault zone, deposits of unit 3 appear to be stratigraphically below units 5 and 6 because unit 3 sediment deposited beneath and around blocks of the older units that were suspended in open fissures, which formed during the most-recent faulting event. The youngest deposit mapped in the trench is a layer of residuum (unit 1) that mantles the modern land surface.

INTERPRETATION OF FAULTING HISTORY

We interpret stratigraphic relations in the trench as recording evidence for three surface-faulting events on the Cheraw fault in Holocene and latest Pleistocene [≤30 k.y. (thousand years)] time. The timing of these events is constrained by four radiocarbon dates on soil organic concentrates and one date on charcoal (table 1 on plate), and nine thermoluminescence (TL) age estimates (table 2 on plate) on samples of silt and fine-grained sand. Reconstruction of paleolandscapes and the thicknesses of pre- and post-faulting deposits help establish general limits on amounts of throw associated with each event (table 3). Finally, we summarize our preferred estimates for the times of these events in table 4.

The four samples of bulk organic material from the buried A horizons and the sample of charcoal from the upper buried A horizon (unit 4pA) yielded stratigraphically consistent radiocarbon age determinations (table 1). The soil organic matter in the buried A horizons is within about 0.5 m of the modern surface and has not been oxidized, which we interpret as direct evidence that the most-recent faulting event is geologically young.
The radiocarbon dates from organic matter in the buried soils must be adjusted for the apparent mean residence time (AMRT) of organic carbon in the A horizons at the time of burial. The accumulation and decomposition of organic matter in A horizons is a dynamic process that ideally reaches a steady state when organic-matter accumulation and decomposition rates are equal (Matthews, 1980). In this steady-state condition, the organic matter remains in the soil for some length of time, which is commonly described as the AMRT (Scharpenseel, 1971). Many factors affect the AMRT of carbon in a soil, including vegetation type, climate, and depth within the soil, and the AMRT can range from hundreds to thousands of years (Paul and others, 1964). In semi-arid regions of the western United States that are climatically similar to southeastern Colorado, the AMRT for a soil is commonly on the order of several hundred years (Machette and others, 1992); that is, a radiocarbon analysis of organics in a modern A horizon would yield an age of several hundred years. For this study, we use 500 years for the AMRT of the soils. For the samples of buried soils listed in table 1, the AMRT is subtracted from the apparent radiocarbon age to better estimate the time when the soil was buried.

Table 3. *Interpretation of amounts of vertical offset on the Cheraw fault, Colorado*

[CW, colluvial wedge. The minimum offset values on the main fault zone for the most-recent and penultimate faulting events are based on the maximum thickness of the colluvium that accumulated at the base of the scarp; these values do not compensate for the effects of any backrotation immediately adjacent to the scarp. The possible offset values on the main fault zone for the most-recent and penultimate events are derived by multiplying the maximum thickness of the colluvial wedge from these events by a factor of two, which is a common way to estimate the height of paleoscarps. The total offset on the secondary fault zone is about 0.8 m, most or all of which occurred during the penultimate faulting event]

Faulting event	Minimum offset on main fault zone	Possible offset on main fault zone	Offset on secondary fault zone	Range of total offset
Most-recent	~0.5 m (maximum thickness of CW).	~1.0 m (twice thickness of CW).	0.0–0.1 m (permissible).	~0.5–1.1 m
Penultimate	~0.4 m (maximum thickness of CW.	~0.8 m (twice thickness of CW).	0.7–0.8 m	~1.1–1.6 m
Oldest	~1.5 m (thickness of distal fill).	~1.5 m (thickness of distal fill).	None	~1.5 m
Total of 3 events.	~2.4 m	~3.3 m	~0.8 m	~3.2–4.1 m

The TL age estimates are from samples of fine-grained deposits that we believe are either primarily in-situ loess or loess that was locally reworked and redeposited on the downthrown side of the scarp. Except for two samples, the TL age estimates are stratigraphically consistent within the error limits of the determinations. The exceptions are samples TL-CF-5 (9.2±0.9 ka) and TL-CF-9 (17.0±1.6 ka). The estimated age of sample TL-CF-5 is anomalously young compared to all of the other TL estimates and radiocarbon ages, most of which are stratigraphically younger. In contrast, sample TL-CF-9 is anomalously old with respect to its stratigraphic position. Based on the radiocarbon ages that stratigraphically bracket sample TL-CF-9, it should have an age between 9.4 ka and 11.2 ka, which is much younger than the TL estimate of 17 ka. Because of their inconsistent ages with respect to stratigraphic and radiometric constraints, we consider the TL age estimate of samples TL-CF-5 and TL-CF-9 to be unreliable, and, therefore, we dismiss them and do not discuss them further in this report.

CUMULATIVE THROW AT THE TRENCH SITE

Two conspicuous zones of normal-slip faults offset stratigraphic units in the trench and juxtapose relatively light-colored fluvial sands (units 7 and 8) against relatively dark-colored silt and clayey silt (units 5 and 6). The faults dip about 70° NW. The main fault zone, which is near the base of the scarp, has a minimum estimated cumulative throw of about 2.4 m (table 3), whereas the secondary, southeastern fault zone has a cumulative throw of only about 0.8 m (table 3). A minor amount of stratigraphic offset is accommodated by gentle tilting between the two faults. Thus, stratigraphic relations in the trench suggest a minimum net throw of about 3.2 m across the entire fault zone.

This minimum net-throw value of about 3.2 m, which is based on the thickness of faulting-related Quaternary deposits adjacent to the fault zones, is comparable to the net throw measured on the top of the Cretaceous bedrock. On the upthrown side of the fault zone, we exposed Smoky Hill Shale Member near the 22-m mark in the trench, and on the downthrown side, we penetrated the shale in auger hole G-1 at a depth of about 4.9 m (fig. 4). Projecting the top of bedrock in the auger hole back to the fault zone and correlating it with the shale exposed in the trench indicates a throw of about 3.2 m (fig. 4).

OLDEST FAULTING EVENT RECORDED IN THE TRENCH

The evidence of the oldest event in the trench is the colluvium and paludal silt (units 5 and 6) that are present only on the downthrown side of the scarp. Prior to this event, a southerly flowing channel (fig. 5), which was part of the area's drainage network, had incised through older Pleistocene alluvium and into the underlying Cretaceous bedrock; the channel was partially filled with fluvial sand and gravel (units 7 and 8). The fault scarp that formed during the oldest event dammed the channel and created a relatively marshy depocenter on the northwest side of the fault. Colluvium from the scarp and paludal silt accumulated in this depocenter. We estimate that about 1.5 m of throw occurred during this faulting event. This estimate is based on a reconstruction of the thickness of the colluvium and alluvium in the distal part of the depocenter, away from the localized backrotation and deformation adjacent to the fault that can exaggerate the thickness of post-faulting deposits.

Table 4. *Interpretation of timing of movements on the Cheraw fault, Colorado*

[^{14}C, radiocarbon; TL, thermoluminescence. Evidence for events that predate the oldest event recorded in the trench is based on the inference that tens of thousands of years would be required for a scarp from older events to be eroded and for a through-flowing drainage channel to be established across any scarp that existed prior to the oldest event recorded in the trench]

Faulting event	Main fault zone	Secondary fault zone	Best estimate of event's age	Type of evidence
Most-recent....	<8.4 ka.....	Probably not active.....	8 ka.....	^{14}C, soil, and stratigraphy.
Penultimate...	<12.1 ka.....	<13.0±1.1 ka, <13.5±1.2 ka.....	12 ka.....	^{14}C, TL, soil, and stratigraphy.
Oldest.....	>18.4±3.9 ka, >21.3±2.5 ka.	Not active (top of bedrock offset same as net offset from events 1 and 2). No stratigraphic evidence of offset.	20–25 ka.....	Stratigraphy and TL.
Older event(s).	_ _	_ _	≥100 ka.....	_ _

All of this throw occurred on the main fault zone; we did not find stratigraphic evidence of vertical movement on the secondary fault zone during this event.

The TL age estimates provide the best constraints on the minimum age of the oldest event. These estimates suggest that unit 6psi has an age of about 18.4–21.3 ka (samples TL-CF-4 and TL-CF-3, respectively, table 2). If we assume that the deposition of unit 6csa and much of 6psi required 2–4 k.y., then the oldest faulting event documented in the trench occurred at about 20–25 ka (table 4). The buried A horizon (unit 5pA) on the paludal silt indicates that a period of relatively slow sedimentation and landscape stability occurred well after the oldest event (recorded in the trench). Organic matter from this soil yielded a conventional radiocarbon age of 10,700±100 yr B.P., which corresponds to a calendric age of about 12,600 yr B.P. (sample C^{14}-CF-2, table 1). We subtract 500 years from this number as the estimated AMRT for soil organic matter, which yields a minimum constraining age of 12.1 ka for the oldest event and a maximum constraining age for the penultimate event.

PENULTIMATE FAULTING EVENT RECORDED IN THE TRENCH

The interval of relatively slow sedimentation on the downthrown side of the fault following the oldest event ended abruptly when the penultimate faulting event rejuvenated the scarp. This rejuvenation accelerated sedimentation on the downthrown side and resulted in deposition of a northwestward-thinning wedge of paludal silt. Following degradation of the scarp from the penultimate event, an A horizon (unit 4pA) and a cambic B horizon (unit 4 pB) formed in this wedge of reworked silt.

Stratigraphic evidence indicates that the total throw from the penultimate event was 1.1–1.6 m (table 3). At the main fault zone, units 4pA and 4pB have a combined thickness of about 0.4 m, which must have been the minimum height of the fault scarp. If we apply a commonly used guideline that the height of a fault scarp is roughly twice the thickness of deposits that accumulated at the base of scarp, then we estimate that the scarp on the main fault zone could have been 0.8 m high. Thus, we use a value of 0.4 m as the minimum vertical offset from this event and 0.8 m as a possible maximum value.

Movement on the secondary fault zone also occurred during this event. The total cumulative throw on the secondary fault is about 0.8 m. The stratigraphic evidence suggests that most, if not all, of this offset occurred during the penultimate event; however, we cannot preclude the possibility that a small amount of throw (<10 cm) occurred during the younger, most-recent event.

The time of the penultimate event is bracketed by radiocarbon ages on organic matter from the A horizon of the two buried soils (units 4pA and 5pA). When this faulting event occurred, deposition of the wedge of paludal silt buried unit 5pA, which has an estimated age of 12.1 ka. Thus the event occurred shortly after 12.1 ka. The age of the A horizon that caps unit 4 establishes a minimum time for the event. This A horizon has an estimated age of 9.4–9.9 ka (samples C^{14}-CF-1, C^{14}-CF-3, and C^{14}-CF-4, table 1). The radiocarbon ages also indicate that the colluvial wedge of paludal silt (unit 4csi) from the penultimate event was deposited over a time span of about 2–3 k.y.

MOST-RECENT FAULTING EVENT RECORDED IN THE TRENCH

The most obvious evidence of the most-recent faulting event on the Cheraw fault is offset of the youngest buried soil (units 4pA and 4pB). This event rejuvenated

the scarp again and resulted in deposition of colluvium and alluvium, which we mapped as units 2 and 3. We estimate that about 0.5–1.1 m of offset occurred during this event (table 3). Most of the offset occurred on the main fault zone, although a small amount of offset could have occurred on the secondary fault zone. If movement did occur on the secondary fault zone, then we suspect that the vertical offset must have been 10 cm or less because a greater offset would have likely left a stratigraphic record of the offset. The maximum thickness of colluvium from this event is slightly less than 0.5 m, which corresponds to the minimum size of the resultant scarp. Doubling this value suggests that the scarp may have been 1.0 m high. If we assume that as much as 0.1 m of offset also occurred on the secondary fault zone, then the cumulative throw during this event could have been 1.1 m.

The radiocarbon dates and TL age estimates only establish a maximum limit on the time of this event because they provide age control only for units that were offset by this event. Three radiocarbon analyses on concentrated organic matter from the buried soil (unit 4pA) that was faulted by this event yielded dates that indicate the most-recent event occurred after 9.4–9.9 ka (table 1). Furthermore, accelerator mass spectrometry (AMS) radiocarbon analysis of charcoal fragments in this A horizon yielded a calibrated age of 8,415 yr B.P. (C^{14}-CF-5, table 1). These charcoal fragments could have been deposited within the A horizon or could have been younger charcoal incorporated into the soil (unit 4pA) prior to its burial by fault-scarp colluvium (unit 2c). Because the age calibration of the charcoal fragments does not require the subjective estimate of AMRT as do soil organics, we have more confidence in the charcoal age compared to the soil ages. Thus, we favor using the charcoal age of 8.4 ka as an estimate of the maximum time for the most-recent faulting event.

We have no absolute ages for deposits (units 1, 2, and 3) that postdate this event, so we cannot define a minimum limit for the time of the event. However, the most-recent event probably occurred within a few hundred years after deposition of the charcoal because we would expect small charcoal fragments located less than 10 cm below the ground surface to be either oxidized or dispersed by bioturbation within a few centuries. Thus, our best estimate for the time of the most-recent event is about 8 ka.

CONCLUSIONS

The Cheraw fault is located on the Piedmont in southeastern Colorado, a region that has been seismically quiescent region during historic time, yet our paleoseismic investigation of the fault indicates that three earthquakes have produced surface rupture during the past 20–25 k.y. and that the most-recent faulting event occurred in the early Holocene. Our study also suggests that the three faulting events on the Cheraw fault may be part of a pattern of temporal clustering of earthquakes in which one or more earthquakes occur in a relatively short period of time (10–15 k.y.), and that this interval of high activity is bounded by long intervals (>100 k.y.) of relative low activity.

Clearly, if significant historical seismicity had been associated with the Cheraw fault, it would have been recognized as a potential source of future large earthquakes. However, recent paleoseismic studies (Crone and Luza, 1990; Kelson and Swan, 1990; Crone and others, 1992; Machette and others, 1993) and historical surface-faulting earthquakes in stable continental regions (Johnston, 1994; Crone and others, in press) show that faults similar to the Cheraw fault can remain aseismic for many thousands of years and rupture unexpectedly with little or no precursory warning. This type of fault behavior indicates that the record of historical seismicity is imperfect in identifying all potentially seismogenic faults in the stable interior of continents.

ACKNOWLEDGMENTS

This study was supported, in part, by a grant from the U.S. Nuclear Regulatory Commission and by the National Earthquake Hazards Reduction Program of the U.S. Geological Survey. We thank Mr. Larry Hansen, President of the Timberlake Grazing Association, for access and permission to excavate the trench on the association's property. Paula B. Maat (formerly of the U.S. Geological Survey) collected the thermoluminescence samples in the field and made the in-situ measurements of radiation for dose rates. We also thank Juan Carlos Moya (University of Colorado, Boulder) and Lin Wei-Hsiung (Central Geological Survey of Taiwan, Taipei) for their assistance in the field during initial studies of the Cheraw fault, and Theodore Barnhard (USGS) and Thomas Machette for assistance in making the detailed topographic survey. In addition, many colleagues and interested geologists gave helpful suggestions during two field trips that we conducted to the site in 1995. However, we accept responsibility for any errors or misinterpretations that exist in this report.

REFERENCES CITED

Bucknam, R.C., and Anderson, R.E., 1979, Estimation of fault-scarp ages from a scarp-height–slope-angle relationship: Geology, v. 7, p. 11–14.

Crone, A.J., and Luza, K.V., 1990, Style and timing of Holocene surface faulting on the Meers fault, southwestern Oklahoma: Geological Society of America Bulletin, v. 102, p. 1–17.

Crone, A.J., and Machette, M.N., 1995, Holocene movement on the Cheraw fault, SE Colorado—Another hazardous late Quaternary fault in the stable continental interior [abs.]: Eos, 1995 Fall Meeting Program, v. 76, no. 46, Nov. 7, 1995/Supplement, p. F362.

Crone, A.J., Machette, M.N., and Bowman, J.R., 1992, Geologic investigations of the 1988 Tennant Creek earthquakes—Implications for paleoseismicity in stable continental regions: U.S. Geological Survey Bulletin 2032–A, 51 p., 2 plates.

——— in press, The episodic nature of earthquake activity in stable continental regions revealed by paleoseismicity studies of Australian and North American Quaternary faults: Australian Journal of Earth Sciences, v. 44, no. 1.

Johnston, A.C., 1994, Seismotectonic interpretations and conclusions from the stable continental region seismicity database, *in* Johnston, A.C., Coppersmith, K.J., Kanter, L.R., and Cornell, C. A., The earthquakes of stable continental regions: Palo Alto, California, Electric Power Research Institute Technical Report TR-102261-V1, p. 4-1–4-103.

Johnston, A.C., and Kanter, L.R., 1990, Earthquakes in stable continental crust: Scientific American, v. 262, p. 68–75.

Kelson, K.I., and Swan, F.H., 1990, Paleoseismic history of the Meers fault, southwestern Oklahoma, and implications for evaluations of earthquake hazards in the central and eastern United States, *in* Weiss, A.J., compiler, Seventeenth water reactor safety information meeting: Washington, D.C., U.S. Nuclear Regulatory Commission, NUREG/CP-0105, p. 341–365.

Kirkham, R.M., and Rogers, W.P., 1981, Earthquake potential in Colorado—A preliminary evaluation: Colorado Geological Survey Bulletin 43, 171 p., 1 plate.

Lowell, T.V., and Teller, J.T., 1994, Radiocarbon vs. calendar ages of major lateglacial hydrological events in North America: Quaternary Science Reviews, v. 13, p. 801–803.

Machette, M.N., Crone, A.J., and Bowman, J.R., 1993, Geologic investigations of the 1986 Marryat Creek, Australia, earthquakes—Implications for paleoseismicity in stable continental regions: U.S. Geological Survey Bulletin 2032–B, 29 p., 1 plate.

Machette, M.N., Personius, S.F., and Nelson, A.R., 1992, Paleoseismology of the Wasatch fault zone—A summary of recent investigations, interpretations, and conclusions: U.S. Geological Survey Professional Paper 1500–A, p. A1–A71.

Madole, R.F., 1994, Stratigraphic evidence of desertification in the west-central Great Plains within the past 1000 yr: Geology, v. 22, p. 483–486.

Matthews, J.A., 1980, Some problems and implications of ^{14}C dates from a podzol buried beneath an end moraine at Haugabreen, southern Norway: Geografiska Annaler, v. 62A, p. 185–208.

Paul, E.A., Campbell, C.A., Rennie, D.A., and McCallum, K.J., 1964, Investigations of the dynamics of soil humus utilizing carbon dating techniques: Transactions, Eighth International Congress of Soil Science, Bucharest, Romania, v. III, p. 201–208.

Scharpenseel, H.W., 1971, Radiocarbon dating of soils—Problems, troubles, and hopes, *in* Yaalon, D.H., ed., Paleopedology—Origin, nature, and dating of paleosols: Jerusalem, Israel, International Society of Soil Science and Israel Universities Press, p. 77–88.

Scott, G.R., 1970, Quaternary faulting and potential earthquakes in east-central Colorado: U.S. Geological Survey Professional Paper 700–C, p. C11–C18.

——— 1982, Paleovalley and geologic map of northeastern Colorado: U.S. Geological Survey Miscellaneous Investigations Map I–1378, scale 1:250,000, 12 p. pamphlet.

Sharps, J.A., 1976, Geologic map of the Lamar [1°x2°] quadrangle, Colorado and Kansas: U.S. Geological Survey Miscellaneous Investigations Map I–944, scale 1:250,000.

Stuiver, Minze, and Reimer, P.J., 1993, Extended ^{14}C data base and revised Calib 3.0 ^{14}C age calibration program: Radiocarbon, v. 35, p. 215–230.